

# Time-Dependent Fluorescence Spectra of Large Molecules in Polar Solvents

Chao-Ping Hsu, Yuri Georgievskii, and R. A. Marcus\*

A. A. Noyes Laboratory of Chemical Physics, 127-72 California Institute of Technology, Pasadena, California 91125

Received: November 19, 1997

A method is described for incorporating the vibronic transitions of a solute molecule in the calculation of the time evolution of its fluorescence spectrum in a polar solvent. In this initial article, systems are treated in which the intramolecular vibrational relaxation is much faster than the observed delay time. The overall fluorescence spectrum is then shown to be a convolution of the steady-state absorption and emission spectra of the solute in a *nonpolar* solvent and the time-dependent emission line shape arising only from polar interactions. Calculations are made for coumarin 153 in acetonitrile, using the dielectric dispersion data of the solvent available from experimental measurements. The results are in encouraging agreement with experimental spectra. Results are also given for the dynamic Stokes shift in methanol.

## 1. Introduction

The dynamics of polar solvents has been studied in charge redistribution processes in many chemical reactions and photo-induced processes.<sup>1–29</sup> Pioneering works, in both theory and experiment in nanosecond time scales, were performed by Bakhshiev, Mazurenko, and their coworkers.<sup>1–4</sup> Experimentally, the time-dependent fluorescence shift (the *dynamic Stokes shift*) has been measured over different time scales and for a variety of polar solvents.<sup>6–15</sup> In typical Stokes shift experiments a chromophoric solute dissolved in a polar solvent is first excited by a pump pulse, and the time-dependent fluorescence spectrum of the solute is then recorded. For studies with coumarin or other dye molecules (e.g., refs 7–15), the excited state of the solute has a charge distribution quite different from that of the ground state. The change in charge distribution causes the polar solvent to adjust its configuration to minimize the interaction free energy. Such processes have been monitored by measuring the dynamics Stokes shift,  $S(t)$ :

$$S(t) = \frac{\nu(t) - \nu(0)}{\nu(\infty) - \nu(0)} \quad (1)$$

where  $\nu(t)$  is either the peak or the averaged frequency of the transient emission spectrum.

It has been shown for coumarin 153 (C153) in polar solvents that such Stokes shift measurements can be described in terms of the polar solvation processes.<sup>9,10,14,15,21,30</sup> For systems with an infinitely short pump pulse,  $S(t)$  is expected to follow the normalized classical correlation function of the interaction energy between the solute and solvent.<sup>29–35</sup> However, when the pulse has a finite duration, it has been shown that the  $S(t)$  is a linear combination of the classical and quantum correlation functions of the interaction,<sup>36</sup> a combination in which the quantum correlation term vanishes in the limit of a very short pump pulse.

Theoretical developments<sup>16–29</sup> have provided much physical insight into solvation dynamics. Solvation correlation functions calculated from the Debye form, the Davidson–Cole and the Cole–Cole forms have been shown to exhibit significant

differences.<sup>16</sup> On the basis of similar calculations and comparisons with experiments, it has been noted that it would be useful to obtain higher frequency dielectric data for a better description of  $S(t)$ , the solvation correlation function.<sup>14</sup>

Much attention has been devoted to treating theoretically the spatial dependence of dielectric response function,  $\epsilon(\mathbf{k}, \omega)$ , which includes the molecular nature of solvent.<sup>19</sup> The dynamical mean spherical approximation theory has been used, for example.<sup>18,20,21</sup> A systematic comparison of the  $S(t)$  predicted by dynamical mean spherical approximation theory with that in experiments was reported in ref 9. It was found there that a slower dynamics is usually predicted by the dynamical mean spherical approximation theory, when the solute is modeled as a dipolar sphere. A molecular hydrodynamic theory<sup>22,23</sup> has been applied to a variety of systems with a model dielectric response function. Agreement between the experimental and calculated solvation correlation function was reported for water,<sup>23,24</sup> alcohols,<sup>25</sup> and acetonitrile.<sup>26</sup> Molecular dynamics calculations have provided information on the influence of polar solvents on the reaction rate<sup>27</sup> and on the role played by various shells of solvent molecules.<sup>16,29</sup> The short-time solvation dynamics has also been interpreted in terms of an *instantaneous normal modes* analysis of molecular dynamics simulations.<sup>28</sup>

The line shape of the time-evolving emission spectrum is considered in the present work. Mukamel and co-workers have developed formal expressions for various optical processes.<sup>37–39</sup> In those works the transient emission spectrum was expressed in terms of a direct summation over all vibronic transitions, in which each transition is described by the time evolution of a single transition between two vibronic states and that evolution was derived from the perturbation theory.<sup>40</sup> Maroncelli and co-workers<sup>9,41,42</sup> and Mazurenko<sup>4</sup> have provided a phenomenological description for estimating the fluorescence at time zero. At the very short time limit, it was assumed that the solvent is frozen but that the internal vibrational relaxation in the solute molecule is already complete. We recall the results here for discussion and application later:

Following Maroncelli and Mazurenko,<sup>4,42</sup> the zero-time fluorescence can be written as proportional to a quantity  $F_P$  given by

$$F_p(\omega, t=0; \omega_{\text{ex}}) = \omega^3 \omega_{\text{ex}} \int_{-\infty}^{\infty} d\omega'' g_{\text{np}}(\omega_{\text{ex}} - \omega'') f_{\text{np}}(\omega - \omega'') p_1(\omega'') \quad (2)$$

where  $g_{\text{np}}(\omega)$  describes the absorption spectrum of the solute molecule and  $f_{\text{np}}(\omega)$  is the emission line shape, both in a nonpolar solvent. The  $p_1(\omega)$  describes the probability distribution of the polar solvent configurations which have a given energy difference  $\hbar\omega$  between the two states of the solute molecule, sampled from the polar solvent configurations in thermal equilibrium with the *ground* electronic state of the solute molecule. Such an energy difference of the two solute electronic states is assumed to arise from the polar solute–solvent interaction. Thus,  $p_1(\omega)$  would have been the absorption line shape in polar solution, if there had been only a difference in the *polar* interactions of the ground- and excited-state Hamiltonians. In applying eq 2, the nonpolar reference absorption and emission spectra are used to obtain  $g_{\text{np}}(\omega)$  and  $f_{\text{np}}(\omega)$ .<sup>9,41,42</sup>

$$\omega g_{\text{np}}(\omega) \propto A_{\text{np}}(\omega) \quad (3)$$

$$\omega^3 f_{\text{np}}(\omega) \propto F_{\text{np}}(\omega) \quad (4)$$

where  $A_{\text{np}}$  is the absorption spectrum and  $F_{\text{np}}$  is the steady-state emission spectrum, for the same solute in a nonpolar reference solvent.

One might imagine that an extension of eq 2 for a phenomenological description of the time-dependent fluorescence can be written as<sup>4</sup>

$$F_p(\omega, t; \omega_{\text{ex}}) = \omega^3 \omega_{\text{ex}} \int_{-\infty}^{\infty} d\omega' \int_{-\infty}^{\infty} d\omega'' \times g_{\text{np}}(\omega_{\text{ex}} - \omega'') f_{\text{np}}(\omega - \omega') p(\omega', t; \omega'') \quad (5)$$

where  $p(\omega', t; \omega'')$  is the time evolution of a probability distribution for the energy difference of the two states of the solute that have a energy difference  $\hbar\omega''$  at  $t = 0$  which then drifts to  $\hbar\omega'$  at time  $t$ , if only polar solute–solvent interactions were included. This drift in the energy difference is due to the difference in charge distributions of solute in the two electronic states. Thus,  $p(\omega', t; \omega'')$  can also be regarded as the time evolution of the emission spectral line shape (with emission frequency  $\omega'$ ) when the pump frequency is  $\omega''$  for the two-state solute if there were only the polar interaction with the solvent. The desired properties of  $p(\omega', t; \omega'')$  are

$$p(\omega', t=0; \omega'') = p_1(\omega'') \delta(\omega' - \omega'') \quad (6)$$

$$\lim_{t \rightarrow \infty} p(\omega', t; \omega'') = p_1(\omega'') p_2(\omega') \quad (7)$$

where the first property is needed to yield eq 2 as a special case of eq 5, and the second property means that at very long time, the spectral shifts  $\omega'$  and  $\omega''$  are independent. The  $p_2(\omega')$  denotes the equilibrium probability distribution of energy difference (spectral shift), sampled from solvent configurations in thermal equilibrium with the *excited*-state solute charge distribution. Thus  $p_2(\omega')$  is also the steady-state emission line shape for the two-state solute when only polar interactions with the solvent are considered.

In the present work it is shown that eq 5 can be obtained from perturbation theory using Mukamel's formalism. The result provides a method for including the vibronic transitions of the dye molecule in the time-dependent fluorescence spectrum. The major physical approximation made is a time separation of the motions. For the purpose of the present article,

the nonpolar interactions between the solute and solvent as well as the intramolecular vibrational motion are treated as instantaneous, while in the literature a Brownian oscillator model is sometimes used.<sup>37,43</sup> The remaining motion is the electrostatic interaction between the solute and the polar solvent. It is assumed to provide all the measurable dynamics in the current upconversion fluorescence experiments.

The outline of the paper is as follows: The general theoretical description of the fluorescence spectrum is presented in section 2.1. The separation of contributions from the above time scales of motion to the interaction energy is made in section 2.2. The results of applying expressions obtained in section 2 to C153 in acetonitrile, using the dielectric continuum model with experimental  $\epsilon(\omega)$  data, are given in section 3. The results are discussed in section 4. It has been pointed out<sup>44</sup> in a treatment of the dynamic Stokes shift that the inclusion of some description of the electronic polarizability of the solute<sup>8,11,45</sup> leads to an improved agreement, and that behavior is also found here. Concluding remarks are given in section 5.

## 2. Theory

### 2.1. General Formalism for the Time Evolution of the Fluorescence Spectrum.

The time evolution of the fluorescence spectrum has been treated by Mukamel and co-workers.<sup>37,38</sup> With their formalism, the time-dependent emission spectrum  $F(\omega, t; \omega_{\text{ex}})$ , the spectral intensity at time  $t$  of the fluorescence at frequency  $\omega$  when the frequency of excitation is  $\omega_{\text{ex}}$  can be calculated from the perturbation theory.<sup>40</sup> The solute molecule is considered to have two electronic states  $|g\rangle$  and  $|e\rangle$ , whose energies are dependent on both the internal vibration coordinates and the configuration of the solvent molecules. Under the Condon approximation, an explicit expression for  $F(\omega, t; \omega_{\text{ex}})$  can be obtained using fourth-order perturbation theory for the interaction between the material and the radiation to calculate the time evolution of the density matrix:<sup>37,38,40</sup>

$$F(\omega, t; \omega_{\text{ex}}) = \left| \frac{E_1 \mu}{\hbar^2} \right|^2 \left| \frac{E_2 \mu}{\hbar^2} \right|^2 \text{Re} \int_{-\infty}^t dt_3 \int_{-\infty}^{t_3} dt_1 \int_{-\infty}^{t_1} dt_2 \times e^{i\omega(t-t_3)} e^{i\omega_{\text{ex}}(t_2-t_1)} e(t_1) e^*(t_2) R(t_1, t_2, t_3; t) \quad (8)$$

where Re denotes the real part of the function,  $E_1$  and  $E_2$  are the electric field strengths of the pump pulse and the emitting light, respectively,  $\mu$  is the transition dipole moment,  $e(t)$  is the profile of the pump pulse, and  $R$  is a four-point correlation function:

$$R(t_1, t_2, t_3; t) = \left\langle \exp_{-\frac{i}{\hbar}} \int_{t_2-t_1}^{t_3-t_1} \chi(\tau_1) d\tau_1 \exp_{+\frac{i}{\hbar}} \int_0^{t-t_1} \chi(\tau_2) d\tau_2 \right\rangle \quad (9)$$

Here,  $\exp_+$  ( $\exp_-$ ) is the time-ordered (reverse-ordered) exponential function,  $\langle \dots \rangle$  indicates that the quantity is averaged over a thermal equilibrium with solute molecule in the *ground state* ( $\equiv \text{Tr}[e^{-\beta H_g} \dots]$ ), and  $\chi$  is the difference in Hamiltonians:

$$\chi = H_e - H_g \quad (10)$$

where  $H_e$  and  $H_g$  are the Hamiltonians for the excited-state and ground-state solute molecule, respectively. They are dependent on both the intramolecular and intermolecular configurations. The  $\chi(\tau)$  in eq 9 is the time evolution of  $\chi$  under the *ground*-state Hamiltonian:

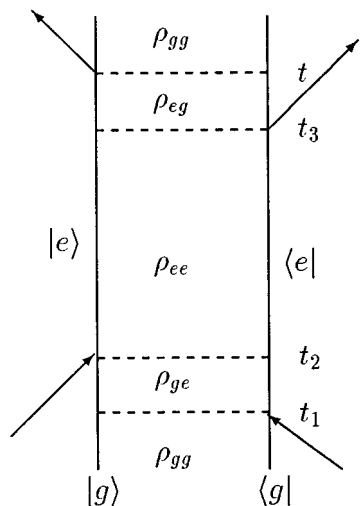


**Figure 1.** Double-sided Feynman diagram for the process of excitation and fluorescence for a two-state system. In this diagram, the density matrix is represented by the two vertical lines. The line on the left represents the ket and the line on the right represents the bra, with time running vertically from bottom to top. An interaction with the radiation field is represented by an arrow. The direction of such an arrow determines the sign of the wave vector contribution to the polarization, which is not explicitly considered in the present study.  $t_1$  and  $t_2$  are any two times occurring during the absorption (pump) pulse. In the integration in eq 8, the excitation times  $t_1$  and  $t_2$  can be reversed.  $t_3$  and  $t$  are the two times when fluorescence occurs.

$$\chi(\tau) = e^{iH_g\tau/\hbar} \chi e^{-iH_g\tau/\hbar} \quad (11)$$

Using the second-order cumulant expansion<sup>46</sup> for  $R$  in eq 9, we have

$$R(t_1, t_2, t_3; t) = e^{i(\Delta G^\circ + \lambda)(t_3 - t + t_1 - t_2)/\hbar} \exp(-1/\hbar^2) [\zeta(t_2 - t_1) + \zeta^*(t - t_3) + \zeta(t - t_1) - \zeta(t_3 - t_1) - \zeta^*(t - t_2) + \zeta^*(t_3 - t_2)] \quad (12)$$

with

$$\zeta(\tau) \equiv \int_0^\tau d\tau_1 \int_0^{\tau_1} d\tau_2 \langle X(\tau_1) X(\tau_2) \rangle \quad (13)$$

$$= \int_0^\tau du (\tau - u) \langle X(u) X(0) \rangle \quad (14)$$

$$X = \chi - \langle \chi \rangle \quad (15)$$

The stationarity of the correlation function  $\langle X(\tau_1) X(\tau_2) \rangle$  was used in obtaining eq 14.

The diagram corresponding to the evolution of density matrix used in obtaining eq 8 is given in Figure 1. In eq 12, the terms  $\zeta(t_2 - t_1)$  and  $\zeta^*(t - t_3)$  are related to the line shapes of the absorption and emission spectra, respectively.<sup>47</sup> The remaining four  $\zeta$  terms in the exponent of  $R(t_1, t_2, t_3; t)$  in eq 12 can be simplified as follows: The ranges of  $t_1$  and  $t_2$  are limited by the excitation pulse profile,  $e(t)$ , while the observation of fluorescence at time  $t$  can be much later. The time  $(t - t_3)$  is limited by the decay time of  $\exp[-\zeta^*(t - t_3)/\hbar^2]$ . For example, for systems at room temperature (such as in ref 9) with a reorganization energy  $\lambda$  of the order  $1000 \text{ cm}^{-1}$  arising from the polar solvation, the decay time for both  $\exp[-\zeta(t_2 - t_1)/\hbar^2]$  and  $\exp[-\zeta^*(t - t_3)/\hbar^2]$  is of the order of 10 fs (cf. eq 27 below). The latter limits  $|t_2 - t_1|$  and  $|t - t_3|$  to be of the order of 10 fs. It is then reasonable to assume, for a simplification of the exponent in eq 12, that

$$0 \approx t_1 \sim t_2 \ll t_3 \sim t \quad (16)$$

Equation 16 implies a significant time difference between the optical absorption (at  $t_1, t_2$ ) during the pulse and the subsequent fluorescence (at  $t_3, t$ ) after the pulse. At the observation time  $t$ , the algebraic sum of the latter four  $\zeta$  terms in eq 12,  $\zeta(t - t_1) - \zeta(t_3 - t_1) - \zeta^*(t - t_2) + \zeta^*(t_3 - t_2)$ , is approximated by a Taylor expansion at time  $t$ , to second order in  $t_1, t_2$ , and  $(t - t_3)$ :

$$\begin{aligned} \zeta(t - t_1) - \zeta(t_3 - t_1) - \zeta^*(t - t_2) + \zeta^*(t_3 - t_2) \approx \\ 2i(t - t_3) \text{Im} \zeta'(t) + (t_2 - t_1)(t - t_3) \text{Re} \zeta''(t) - \\ i(t_2 + t_1 + t - t_3)(t - t_3) \text{Im} \zeta'''(t) \quad (17) \end{aligned}$$

where the primes denote the first and second derivatives of  $\zeta(t)$ , and Re and Im denote the real part and imaginary part of the functions, respectively.<sup>48</sup> The first term in the right-hand side of eq 17 is the leading term of the algebraic sum of the four  $\zeta$  functions. It results in a spectral shift in the Fourier transform to the frequency domain. Thereby, those four  $\zeta$  functions in the exponent of eq 12 generate the time-dependent spectral shift, among other (higher order) effects.

In the next section, we describe a way of treating the intramolecular vibrational modes of the solute molecule.

## 2.2. Treatment of the Internal Vibrational Relaxation.

For a polar molecular such as C153 in a polar solvent, the ground-state and excited-state energies have a different dependence on the internal vibration coordinate and on the solvent configuration. The solvent part can be considered to be composed of both nonpolar and polar interactions. The nonpolar interaction arises, in part, from any difference in size or shape of the wave functions of the two electronic states, and the polar part arises from the electrostatic interaction of the solvent polarization with the different charge distribution of the ground and excited states of the solute molecules. Thereby,  $X$  can be divided into two parts:

$$X = X_s + X_f \quad (18)$$

where  $X_f$  arises from the intramolecular vibrations of the solute and the van der Waals type of nonpolar interaction between the solute and solvent, both treated here as fast.  $X_s$  is the part of energy difference arising from the electrostatic interaction between the solute and polar solvent, which then provides the major contribution to the dynamic Stokes shift and is assumed to respond more slowly than the  $X_f$  for the present study. For studies with higher time resolution or for other solutes and solvents, the assumption that the  $X_f$  response is instantaneous can be removed by using a model, Brownian oscillators for example,<sup>37,43</sup> and we may do so later for a related problem.

Assuming  $X_f$  and  $X_s$  to be statistically independent, the correlation function in  $X$  can be separated as

$$\langle X(\tau_1) X(\tau_2) \rangle = \langle X_f(\tau_1) X_f(\tau_2) \rangle + \langle X_s(\tau_1) X_s(\tau_2) \rangle \quad (19)$$

The corresponding  $\zeta$  function becomes

$$\zeta(t) = \zeta_f(t) + \zeta_s(t) \quad (20)$$

For the fast modes,  $\langle X_f(t) X_f(0) \rangle$  is assumed to decay to zero before the fluorescence is observed in the experiment. Namely, we approximate the correlation function arising from such fast motions by its long time limit. Thereby, the fast mode contribution to the right-hand side of eq 17 yields  $2i(t - t_3)\lambda_f/\hbar$  arising from the first term, and zero from the other two terms,

where  $\lambda_f$  is

$$\lambda_f \equiv -(1/\hbar) \lim_{t \rightarrow \infty} \text{Im} \zeta'_f(t) \\ = -(1/\hbar) \int_0^\infty \text{Im} \langle X_f(t) X_f(0) \rangle dt \quad (21)$$

[The second equality in eq 21 can be seen from the definition of  $\zeta(t)$  in eq 13.] With the above definition,  $\lambda_f$  is the reorganization energy arising from the fast modes.<sup>49</sup> This fast-mode contribution,  $2i(t - t_3)\lambda_f/\hbar$ , yields a constant spectral shift  $2\lambda_f/\hbar$  in the emission frequency  $\omega$  when introduced into eqs 12 and 8.

In rewriting the time-dependent fluorescence  $F(\omega, t; \omega_{\text{ex}})$  in eq 8 with the separation of fast and slow modes, eq 20 is used for all six  $\zeta$  functions in eq 12. The approximation given in eq 17 is used, with the terms for fast modes being simplified as described above, and the result is used to rewrite  $F(\omega, t; \omega_{\text{ex}})$  in eq 8. Such manipulation is followed by a rearrangement of the various terms in the exponent. Equation 8 can then be rewritten as

$$F(\omega, t; \omega_{\text{ex}}) \propto \text{Re} \int_{-\infty}^\infty dt' \int_{-\infty}^\infty dt'' e^{i\Delta\omega t'} e^{i\Delta\omega_{\text{ex}} t''} \times \\ \theta(\tau') \tilde{g}(\tau'') \tilde{f}(\tau') \tilde{p}(\tau', t; \tau'') \quad (22)$$

where  $\Delta\omega \equiv \omega - (\Delta G^{\text{solv}} + \lambda_s)/\hbar$ ,  $\Delta\omega_{\text{ex}} \equiv \omega_{\text{ex}} - (\Delta G^{\text{solv}} + \lambda_s)/\hbar$  and  $\tilde{g}$ , and  $\tilde{f}$  and  $\tilde{p}$  are defined below. The equilibrium free energy difference  $\Delta G^\circ$  of the two states in a polar solvent has been written as the sum of the free energy difference in a *nonpolar* solvent,  $\Delta G_{\text{np}}^\circ$ , and the difference in the solvation free energy  $\Delta G^{\text{solv}}$  between the ground and excited states of the solute. In obtaining eq 22 from eq 8, with  $\tilde{p}$  defined below by eq 25, a change of variables has been introduced:  $\tau' \equiv t - t_3$ ,  $\tau'' \equiv t_2 - t_1$ , and (for eq 25)  $u \equiv t_1 + t_2$ .  $\theta(\tau)$  is a step function that equals 1 if  $\tau \geq 0$  and 0 otherwise. This step function is introduced so that the range of integration over  $\tau'$  becomes  $-\infty$  to  $\infty$  instead of 0 to  $\infty$ , and so the convolution theorem of Fourier transform can then be applied.<sup>50</sup> The  $\lambda_s$  is the reorganization energy arising from the “slow modes”, with a definition analogous to that in eq 21, but for the slow variable,  $X_s(t)$ .

The functions  $\tilde{f}(\tau')$  and  $\tilde{g}(\tau'')$  in eq 22 describe the fast-mode contribution, and  $\tilde{p}(\tau', t; \tau'')$  contains the slow-mode contribution and the optical pulse shape. These functions are given by

$$\tilde{f}(\tau') \\ \equiv \exp[-\zeta_f^*(\tau')/\hbar^2 + 2i\tau'\lambda_f/\hbar] \exp[-i(\Delta G_{\text{np}}^\circ + \lambda_f)\tau'/\hbar] \\ = \exp[-\zeta_f^*(\tau')/\hbar^2 - i(\Delta G_{\text{np}}^\circ - \lambda_f)\tau'/\hbar] \quad (23)$$

$$\tilde{g}(\tau'') \equiv \exp[-\zeta_f(\tau'')/\hbar^2 - i(\Delta G_{\text{np}}^\circ + \lambda_f)\tau''/\hbar] \quad (24)$$

$$\tilde{p}(\tau', t; \tau'') \equiv \int_{-\infty}^\infty du e^{\left(\frac{u - \tau''}{2}\right)} e^{\left(\frac{u + \tau''}{2}\right)} \times \\ \exp(-1/\hbar^2) [\zeta_s^*(\tau'') + \zeta_s^*(\tau') + 2i\tau' \text{Im} \zeta'_s(t) + \\ \tau' \tau'' \text{Re} \zeta''_s(t) - i(u + \tau')\tau' \text{Im} \zeta''_s(t)] \quad (25)$$

Expressions in eqs 23 and 24 are, respectively, the Fourier transforms of the long-time emission and absorption spectra that the system would have in the absence of the slow-mode (electrostatic) interaction.<sup>51,52</sup> These spectra can be approximated by the steady-state absorption and emission spectra of the same solute molecule in a *nonpolar* solvent. Application of the convolution theorem to eq 22 then yields

$$F(\omega, t; \omega_{\text{ex}}) \propto \int_{-\infty}^\infty d\omega' \int_{-\infty}^\infty d\omega'' \times \\ g(\omega_{\text{ex}} - \omega'') f(\omega - \omega') p(\omega' - \omega_0, t; \omega'' - \omega_0) \quad (26)$$

with  $\omega_0 \equiv (\Delta G^{\text{solv}} + \lambda_s)/\hbar$ . The equation above is of the form given by eq 5. The factors  $\omega^3$  and  $\omega_{\text{ex}}$  are obtained by summing over the emission photon mode and converting the number of absorption photons into energy units.<sup>53</sup>

To integrate eq 25 for the purposes of the present paper, a Gaussian optical pulse,  $e(t) \sim \exp(-t^2/\tau_p^2)$ , is assumed, though this assumption is a convenience rather than a necessity. When the Gaussian approximation<sup>54</sup>

$$\exp(-1/\hbar^2) \zeta_s(t) \approx \exp(-\lambda_s k_B T t^2/\hbar^2) \quad (27)$$

is used to obtain the Fourier transform of  $\tilde{p}(\tau', t; \tau'')$ , the result of these manipulations yields

$$p(\omega', t; \omega'') \propto \frac{1}{\sqrt{A(t)}} \exp\left[-\frac{B(t)^2}{4A(t)} - \frac{\omega''^2}{C}\right] \quad (28)$$

where

$$A(t) = \frac{\lambda_s k_B T}{\hbar^2} - \frac{\text{Re} \zeta''_s(t)^2}{2C\hbar^4} \quad (29)$$

$$B(t) = \omega' + 2 \text{Im} \zeta'_s(t)/\hbar^2 + \omega'' \frac{\text{Re} \zeta''_s(t)}{C\hbar^2} \quad (30)$$

$$C = \frac{2\lambda_s k_B T}{\hbar^2} + \frac{1}{\tau_p^2} \quad (31)$$

where the  $\text{Im} \zeta''_s(t)$  ( $=\text{Im}\langle X_s(t) X_s(0) \rangle$ ) is neglected because the imaginary part of the correlation function is much smaller than the real part. Moreover, in eq 25,  $\text{Im} \zeta''_s(t)$  is multiplied by factors composed of  $u$  and  $\tau'$ , and they are limited by the pump pulse profile and the decay time of  $\exp[-\zeta_s^*(\tau')/\hbar^2]$ , respectively. The latter is of the same order as the  $\tau'\tau''$  in eq 25. From eq 25 it can be inferred that the function  $p(\omega', t; \omega'')$  is the time evolution of the emission spectrum (with emission frequency  $\omega'$ ) for a two-state solute that is excited at frequency  $\omega''$ , if only  $X_s$  contributed to the difference in the Hamiltonians of the two states. (Cf. the general expression for time-evolution emission spectrum in eq 8.)

Thereby, the time-dependent fluorescence spectrum can be calculated from the convolution of the steady-state absorption and emission spectra in a nonpolar solvent and the function  $p(\omega', t; \omega'')$  given by eq 28. To calculate  $p(\omega', t; \omega'')$ , the explicit numerical values of the integrated correlation function  $\zeta_s(t)$  are needed. They can be obtained from the correlation function  $\langle X_s(t) X_s(0) \rangle$  using eq 14.

For treating the correlation function, several approaches come to mind. One involves using, in effect, linear response theory, as Ovchinnikov and Ovchinnikova did<sup>55</sup> in their application of a quantum field theoretic method.<sup>56</sup> This treatment does not use a molecular harmonic oscillator model.<sup>57</sup> In a work by Mukamel,<sup>58</sup> a spectral density function  $J(\omega)$  was introduced from a general consideration that involves large anharmonic vibrations of molecules. A property of such a spectral density function was also discussed in the context of the fluctuation–dissipation theorem there.<sup>58</sup> From such a property, the correlation function can be written in terms of its corresponding spectral density in the frequency domain:<sup>58,59</sup>

$$\langle X_s(t) X_s(0) \rangle = \frac{\hbar}{\pi} \int_0^\infty d\omega J(\omega) \left( \coth \frac{\beta \hbar \omega}{2} \cos \omega t - i \sin \omega t \right) \quad (32)$$

where  $\beta \equiv 1/k_B T$ . Even though the terms inside the parentheses of the integrand resemble the correlation function of a harmonic oscillator,<sup>60</sup> eq 32 is obtained from a general consideration of the properties of correlation functions and is not limited to any harmonic oscillator model.<sup>55,58,59</sup>

The spectral density  $J(\omega)$  can be related to a measurable property of the solvent, the dielectric dispersion  $\epsilon(\omega)$ . With the simple continuum model, the linear response theory can be applied to obtain the response function for a time-varying dipole representing the solute. Such response function is closely related to the correlation function  $\langle X_s(t) X_s(0) \rangle$  needed here.<sup>59,61</sup> In ref 55 a homogeneous boundary condition was implicitly assumed and a form of  $J(\omega)$  in terms of  $\epsilon(\omega)$  was obtained. For a point dipole in a sphere cavity model, the spectral density  $J(\omega)$  is<sup>37,62</sup>

$$J(\omega) = -\frac{2\Delta\mu^2}{a^3} \text{Im} \left[ \frac{\epsilon(\omega) - 1}{2\epsilon(\omega) + 1} \right] \quad (33)$$

where  $\Delta\mu$  is the change in the dipole moment of the solute in the two states, and  $a$  is the radius of the cavity. For a spherical cavity filled with dielectric material having a dielectric constant  $\epsilon_c$  to account for the electronic polarizability of the solute, the corresponding expression is (compare related expressions in refs 8, 11, 45, and 63–65)

$$J(\omega) = -\frac{2\Delta\mu^2}{a^3} \text{Im} \left[ \frac{\epsilon(\omega) - 1}{2\epsilon(\omega) + \epsilon_c} \right] \left( \frac{\epsilon_c + 2}{3} \right) \quad (34)$$

which reduces to eq 33 when  $\epsilon_c$  is assumed to be unity.

The correlation function of  $X_s$  can now be obtained using the above expressions for  $J(\omega)$  and eq 32. The integrated correlation function  $\zeta_s(t)$  is then, from eq 14, given by

$$\zeta_s(t) = \frac{\hbar}{\pi} \int_0^\infty d\omega \frac{J(\omega)}{\omega^2} \left[ \coth \frac{\beta \hbar \omega}{2} (1 - \cos \omega t) - i(\omega t - \sin \omega t) \right] \quad (35)$$

Two functions needed in eqs 29 and 30 to calculate the time-dependent fluorescence spectrum are<sup>66</sup>

$$\text{Im} \zeta'_s(t) = \frac{\hbar}{\pi} \int_0^\infty d\omega \frac{J(\omega)}{\omega} (-1 + \cos \omega t) \quad (36)$$

$$= -\lambda_s \hbar + \frac{\hbar}{\pi} \int_0^\infty d\omega \frac{J(\omega)}{\omega} \cos \omega t \quad (37)$$

$\text{Re} \zeta''_s(t) = \text{Re} \langle X_s(t) X_s(0) \rangle =$

$$\frac{\hbar}{\pi} \int_0^\infty d\omega J(\omega) \coth(\beta \hbar \omega / 2) \cos \omega t \quad (38)$$

They can be calculated using Fourier cosine transform subroutines. The second term of eq 37, if normalized to unity at  $t = 0$ , is the same as the function  $\Delta(t)$  used in ref 36 and has been shown to be  $S(t)$ , the dynamic Stokes shift function.<sup>30</sup> Namely

$$S(t) = \frac{\int_0^\infty \cos \omega t J(\omega) / \omega d\omega}{\int_0^\infty J(\omega) / \omega d\omega} \quad (39)$$

The term  $\text{Re} \zeta''_s(t)$ , when normalized, yields  $\Delta_1(t)$  in our previous work.<sup>36</sup>

### 3. Application

Using experimental data for  $\epsilon(\omega)$  for the solvents, all the correlation functions of the solvent modes needed can be calculated with the aid of eqs 33 (or 34), 37, and 38. The overall spectral line shape can be then obtained from eqs 26 and 28.

The dielectric dispersion  $\epsilon(\omega)$  of acetonitrile has been measured for a wide frequency range. At low frequencies, Barthel et al. reported parameters for a Cole–Cole equation for frequencies lower than 89 GHz,<sup>67,68</sup> which corresponds roughly to  $3 \text{ cm}^{-1}$ . In the microwave and far-infrared region (frequencies up to 200 or 250  $\text{cm}^{-1}$ ) the optical constants (complex refractive indexes) have been reported.<sup>69–72</sup> The absorption peak at about 378  $\text{cm}^{-1}$  was measured and described in ref 73. For the infrared region, there is the early work by Goplen et al.<sup>74</sup> and Bertie's recent work.<sup>75</sup>

For the present calculation, the parameters of Cole–Cole equation in ref 67 are used for the low-frequency region. For frequencies higher than 3  $\text{cm}^{-1}$ , we first obtain the imaginary part  $k(\tilde{\nu})$  of the complex refractive index ( $\hat{n}(\tilde{\nu}) = n(\tilde{\nu}) - ik(\tilde{\nu})$ ) from data in the literature.<sup>70,73,75,76</sup> The absorption coefficients  $\alpha(\tilde{\nu})$  reported in refs 70 and 73 can be converted to  $k(\tilde{\nu})$  by dividing  $\alpha$  by  $2\pi\tilde{\nu}$ . A cubic spline interpolation<sup>77,78</sup> was then used to obtain  $k(\tilde{\nu})$  for any given frequency. The Kramers–Kronig transformation<sup>79</sup> was used to obtain the real part of refractive index,  $n(\tilde{\nu})$ , from  $k(\tilde{\nu})$ :

$$n(\tilde{\nu}) = n_\infty + \frac{2}{\pi} P \int_0^\infty \frac{\tilde{\nu}' k(\tilde{\nu}') d\tilde{\nu}'}{\tilde{\nu}'^2 - \tilde{\nu}^2} \quad (40)$$

where  $P$  denotes the principal value of the integral, and the upper limit “ $\infty$ ” denotes an optical frequency, where  $n = n_\infty$ . It has been shown<sup>80</sup> that to obtain  $n(\tilde{\nu})$  at infrared frequencies by integrating over  $k(\tilde{\nu})$  in only the infrared region, the above equation can be rewritten as

$$n(\tilde{\nu}) \approx (a_0 + a_2 \tilde{\nu}^2 + a_4 \tilde{\nu}^4) + \frac{2}{\pi} P \int_0^{\tilde{\nu}_{\text{IR}}} \frac{\tilde{\nu}' k(\tilde{\nu}') d\tilde{\nu}'}{\tilde{\nu}'^2 - \tilde{\nu}^2} \quad (41)$$

where the first three terms in parentheses are a suitable approximation to the contribution from the UV absorption. For the present calculation, coefficients ( $a_0$ ,  $a_1$ , and  $a_2$ ) are obtained from those given in ref 80. The numerical integration using eq 41 gives an  $n(\tilde{\nu})$  in good agreement with the values reported in refs 70, 75, and 81. The dielectric dispersion  $\epsilon(\omega)$  for those frequencies equals the square of the complex refractive index,  $n(\tilde{\nu}) - ik(\tilde{\nu})$ , and so is now known.

The values of  $\text{Im} \zeta'_s(t)$  and  $\text{Re} \zeta''_s(t)$  are obtained using the dielectric dispersion data obtained above and eqs 33 (or 34), 37, and 38. The nonpolar reference spectra are those published in ref 9 for C153 in 2-methylbutane. In the calculation we also need a number for  $(\Delta G^{\text{sol}} + \lambda_s)/\hbar$ , which is the change in absorption frequency due to a change in solvent polarity. This quantity for a polar molecule is dependent on solvent polarity and the dipole moments of both states of the molecule (cf. eq 20 of ref 30 or eq 4.2 of ref 9). In the present work 1490  $\text{cm}^{-1}$  is used for this quantity,  $(\Delta G^{\text{sol}} + \lambda_s)/\hbar$ , for C153 in acetonitrile.<sup>82</sup>

The overall spectral shift due to the polar interaction is  $2\lambda_s$ , which is proportional to the factor  $\Delta\mu^2/a^3$  in eqs 33 and 34. Maroncelli and Fleming have examined the steady-state Stokes shift measurements of C153 in various polar solvents and have

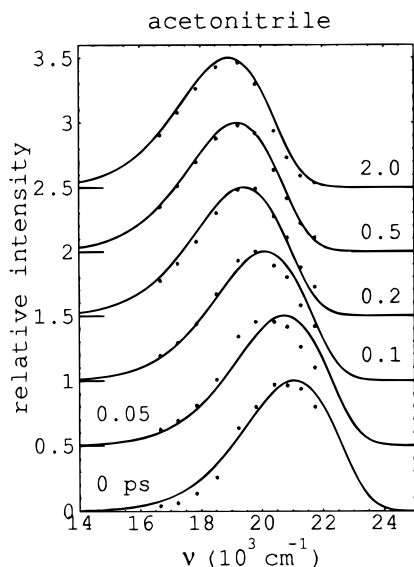


**Figure 2.** Calculated time-dependent emission spectra for coumarin 153 in acetonitrile at different delay times (solid lines) and the experimental data (dots inferred from the figures in ref 10). The delay times are indicated in the units of picosecond. Baselines for different delay times are shifted vertically and are indicated at the left of the figure.

obtained the dipole moment change as 6.0 D if the radius of the spherical cavity resembling the solute molecule is assumed to be 3.9 Å.<sup>8</sup> From fitting the emission spectral position calculated at  $t \rightarrow \infty$  to the steady-state experimental fluorescence spectrum, we obtained a similar value, 6.1 D, as the dipole moment change for a nonpolarizable solute of the same size. However, if a polarizable spherical solute model is used (eq 34), the size of the calculated dipole is smaller for the given solvation free energy: Assuming  $\epsilon_c = 2.0$ ,<sup>11</sup> the dipole moment change is estimated to be 5.1 D from the same resulting  $\lambda_s$  as that calculated using the nonpolarizable model with  $\Delta\mu = 6.1$  D.<sup>83</sup> Using this  $\epsilon_c$  and  $\Delta\mu$  for the polarizable model, the result of the overall calculation for the time-dependent emission spectrum is compared in Figure 2 with the experimental spectrum obtained from ref 10. In the calculation we set  $\tau_p = 50$  fs, which corresponds to 118 fs fwhm in the correlation between pulses. (The values of 112–125 fs is reported in ref 10.) In Figure 3 the dynamic Stokes shift  $S(t)$ , calculated from the second term of eq 37, is plotted together with that obtained from experiment.<sup>9</sup>

We have also calculated a dynamic Stokes shift for methanol: Dielectric dispersion data for methanol are available for a wide range of frequencies. The parameters obtained from fitting microwave measurements to a three-term Debye model have been reported for frequencies less than 295 GHz ( $\approx 10$  cm<sup>-1</sup>).<sup>84</sup> The complex refractive indexes of methanol from 2 to 8000 cm<sup>-1</sup> have been reported in ref 85. For frequencies from 2 to 50 cm<sup>-1</sup>, the dielectric dispersion was also measured by Kindt et al.<sup>86</sup> A three-term Debye model fit was performed in the latter work, and the dielectric dispersion results obtained from those parameters agree fairly well with the lower frequency results reported by Bertie.<sup>85</sup> For the present calculation a cubic spline fit of the tabulated numbers from Bertie's work was used for frequencies higher than 8 cm<sup>-1</sup>. For frequencies lower than 8 cm<sup>-1</sup> the three-term Debye fit reported in ref 84 was used.

The calculated  $S(t)$  is compared in Figure 4 with the experimental results of ref 9. In this case the plot from dipole in a spherical cavity model is seen to deviate from that from experiment. Results from a calculation using the polarizable

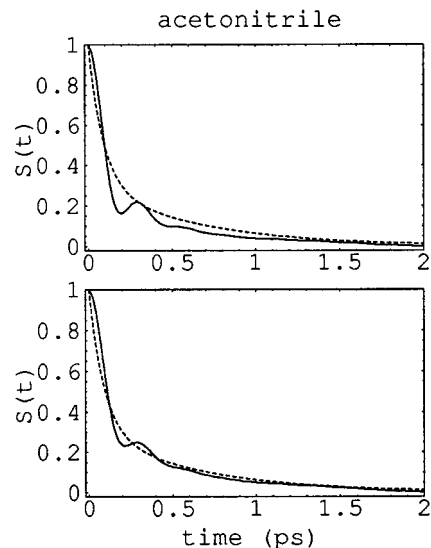


**Figure 3.** Top panel: the dynamic Stokes shift  $S(t)$  for acetonitrile calculated using eq 33 (solid line) and the results fitted to experimental data<sup>9</sup> (dashed line). Bottom panel: calculated  $S(t)$  using eq 34 (solid line) with  $\epsilon_c = 2$  and the same experimental results (dashed line).

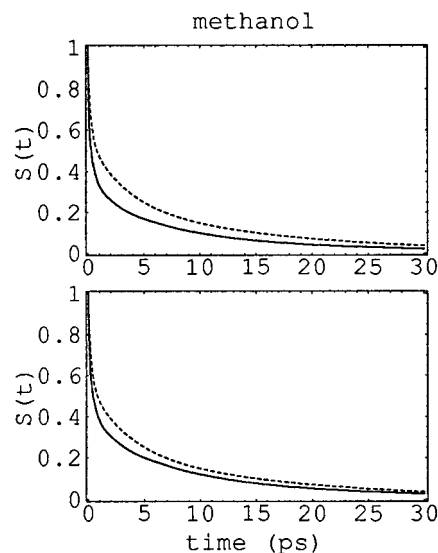


**Figure 4.** Top panel: the dynamic Stokes shift  $S(t)$  for methanol calculated using eq 33 (solid line) and the results fitted to experimental data<sup>9</sup> (dashed line). Bottom panel: calculated  $S(t)$  using eq 34 (solid line) with  $\epsilon_c = 2$  and the same experimental results (dashed line).

solute model using eq 34 with the cavity dielectric constant  $\epsilon_c = 2$  are also given in Figure 4, and the agreement is seen to be somewhat improved.

#### 4. Discussion

There is seen to be reasonably good agreement in Figure 2 between the position and spectral shapes of the calculated time-dependent spectra in acetonitrile and those from experiment, when the possible experimental uncertainties are considered, especially at early times.<sup>32</sup> This result supports the idea that the dynamics observed is mainly relaxation from the polar interaction between the solute and the solvent. In a recent article on shorter times<sup>87</sup> the authors reported very early transient absorption and gain (spontaneous emission) spectra after a pump pulse of C153 in acetonitrile and methanol. At short those times ( $\leq 300$  fs) the gain band is red-shifted with two isosbestic points appearing successively. It has been noted<sup>87</sup> that such results

may imply that some intramolecular process is involved in the earlier dynamics.

The time dependence of the emission spectrum in polar solutions has long been a subject of interest. In the 1960s and 1970s, experiments were performed on the nanosecond time scale,<sup>3,65</sup> and the *kinetics* of the spectrum was discussed in terms of the lifetime of the excited state and the orientational relaxation of the solvent molecules. The latter was related to the dielectric dispersion,  $\epsilon(\omega)$ ,<sup>1,2</sup> and a Debye form was used for  $\epsilon(\omega)$  to account for the orientation dipole relaxation.<sup>1–3,65</sup> A stochastic theory was also proposed to describe the time evolution of the spectrum<sup>4</sup> (cf. recent work by Maroncelli and co-workers<sup>41,42</sup>). As the techniques advanced, the dynamics in the femtosecond time regime became observable, and so a relaxation in the intermolecular vibrations (e.g., the librational mode for water<sup>13,30</sup>) has become important in understanding the experimental results in that time region. The low-frequency intramolecular vibrations in both solute and solvents may also affect the early time evolution. By including in the dielectric dispersion the IR frequency region, we have taken the solvent vibrational modes into account.

In the present work we have considered the case, in deriving the expressions used in calculations, that the vibrational relaxation is complete before the time of observing fluorescence. A short-range nonpolar interaction and the relaxed vibrational contribution were included in an approximate way, by using the absorption and emission spectra in a *nonpolar* solvent. For experiments with a higher time resolution or with techniques that are more sensitive to short-time dynamics, the solute vibrational relaxation should be considered explicitly. In the present case, it was found in ref 9 that almost no time dependence of the spectral shift is observed in their observations on the fluorescence of C153 in 2-methylbutane and that the transient fluorescence spectrum is very close to that of the steady-state fluorescence spectrum for the same system (all are Stark-shifted from the absorption spectral maximum). This result shows that in this nonpolar solvent the relaxation to equilibrium free energy of the excited state occurs within the time resolution (120 fs fwhm instrumental response<sup>9</sup>) of the experiment and so supports the assumption of fast relaxing internal modes made in the present study. The assumption itself provides a major simplification and permits the simple application of expressions for a two-level problem to a real system.

In the present calculation, there are two undetermined quantities that are inferred from experimental spectra. One is  $(\Delta G^{\text{sol}} + \lambda_s)/\hbar$ , the difference between averaged absorption spectra in polar and in nonpolar solvents. For the present study, a value of this quantity was chosen so as to yield agreement between the calculated and the reported (estimated) zero-time fluorescence spectrum in ref 10. The other undetermined quantity,  $\Delta\mu^2/a^3$ , is proportional to  $\lambda_s$  and so is proportional to the overall dynamic spectral shift. The latter is also related to the width of  $p(\omega', t; \omega'')$  (eq 29). However the width of this  $p(\omega', t; \omega'')$  has only a small influence on the line shape of final convoluted spectrum,  $F(\omega, t; \omega_{\text{ex}})$ , because of the large Franck–Condon vibrational contribution to the width. Thereby, the quantity  $\Delta\mu^2/a^3$  can be estimated solely from the spectral shift arising from the polar interaction, namely, the frequency difference of the zero-time emission spectrum and the steady-state fluorescence spectrum in the polar solvent. With the nonpolarizable model, the change in dipole moment is estimated to be 6.1 D, using the peak frequency difference of the zero-time estimated emission spectrum and the steady-state emission spectrum in methanol reported in refs 32 and 9, respectively.

This result agrees, as noted earlier, with the 6.0 D estimated in ref 8 from the steady-state experimental spectrum using the same nonpolarizable model.

The calculated dynamic Stokes shift result for acetonitrile, shown in Figure 3, has an oscillation period of about 0.3 ps, which arises from a strong far-infrared absorption at about  $100 \text{ cm}^{-1}$ . The results in Figure 3 with polarizable solute are quite close to those reported in a recent work,<sup>88</sup> calculated from a theory that the authors developed for the longitudinal linear dielectric response of polarizable solvents with given shape and charge distribution. (That theory includes a  $k$  spatial dependence.) No such oscillation is reported in the experimental data, but the latter depend on the time resolution of the technique and the data processing used. In ref 9 it is indicated that the deconvolution of an instrumental response function has been performed on the raw emission intensity data. It would be interesting to see if such an oscillatory correlation function can be observed in experiments with finer time resolution, such as that in photon echoes.<sup>89</sup>

The dynamic Stokes shift results for methanol are shown in Figure 4 and display an appreciable discrepancy when compared with experiment.<sup>9</sup> It is seen there that the inclusion of  $\epsilon_c$  to represent polarizability of solute improves somewhat the agreement of experiment and theory.<sup>11,44</sup> Since we use the simple dielectric continuum in describing the solvent and extend the frequency range to include IR frequencies, the entire response of the *bulk* solvent to a change in electric field is considered. Using other theoretical methods, namely, the dynamical MSA theory and the molecular hydrodynamic theory, the following results have been obtained for polar solvents:

In ref 9 it was shown that in the case of methanol, a calculated  $S(t)$  using a model for the dielectric dispersion with the far-infrared dielectric response included is significantly faster than measured dynamic Stokes shift from experiment. In the same work the authors compared the dynamics calculated from the dynamical MSA theory,<sup>18</sup> which includes a spatial-dependent dielectric response, with the experimental  $S(t)$ . They concluded that the dynamical MSA theory gives results that are slower than those from a simple continuum model which is used in the present work. For most of the cases studied in ref 9, the dynamical MSA theory predicts a dynamical behavior slower than the experimental one for C153 if a dipolar hard sphere is used to represent the solute. On the other hand, when the neutral dipolar solute was modeled as an ion, an improved agreement was obtained in applying the dynamical MSA theory. However, a charge distribution appropriate to the actual one should of course be used in comparing with the experimental  $S(t)$ .

In a recent article, Bagchi and co-workers applied their molecular hydrodynamic theory, which includes rotational and translational contributions of solvent polarization relaxation, to monohydroxy alcohols.<sup>25</sup> They reported the calculated *dipolar* solvation to be slightly slower than the experimental observation. Again, when the neutral dipolar C153 solute is hypothetically modeled as an ion in their model calculations, there is better agreement between the calculated and experimental  $S(t)$ .<sup>25</sup>

We have investigated the effect of pulse width by changing the pulse duration  $\tau_p$  of Gaussian pulses from the limit of very short pulses to the limit of pulses that are much longer than the dephasing time ( $\hbar/\sqrt{\lambda_s k_B T}$ ) (but still shorter than the fluorescence observation time), by taking the limits of small and large  $\tau_p$  in the expressions in eqs 29 and 30. Results of calculations of these two limiting cases showed negligible changes in the widths in the emission spectra (of the order of  $10 \text{ cm}^{-1}$  for acetonitrile). The small effect of the pulse widths can be

understood as follows: As shown in section 2.2 and eq 26, the overall time-dependent spectrum is a convolution of  $p(\omega', t; \omega'')$  and the steady-state absorption and emission spectra in a nonpolar solvent. The absorption and emission spectra in the nonpolar solvent have a large width, largely due to the quantized in-plane aromatic ring vibrations, which serve as a frame for the spectra that is filled in by absorption or emission due to the lower frequency modes. While in a more detailed study the correct shape of pulse profile could be used and it may lead to a change in  $p(\omega', t; \omega'')$  (eq 25), it is not expected to be able to change the overall spectrum  $F(\omega, t; \omega_{\text{ex}})$  significantly after the convolution with the large-width reference nonpolar absorption and emission spectra.

For the same reason, the line-shape information obtained from the function  $p(\omega', t; \omega'')$  is mostly buried in the convolution with the large-width reference spectra. As seen in eqs 28 and 29, the spectral evolution of a single transition has its spectral width controlled by the quantum correlation function (the expression in eq 38). However, after convolution with the broad reference absorption and emission spectra, the effect of spectral width of a single transition is quite small in the final result. Thus, the quantum solvent effect cannot be easily retrieved from the final spectral line shape for such systems. The time evolution of the fluorescence spectral bandwidths were measured and reported for C153 in dimethyl sulfoxide (DMSO)<sup>9</sup> and for 1,1',3,3,3',3'-hexamethylindotricarbocyanine (HITC) in ethanol.<sup>90</sup> With the advances in techniques in obtaining data with an improved time resolution and with a continuum spectral measurement, it should be possible to address more closely the evolution of emission bandwidth and other details of the line shape in terms of solvation dynamics and molecular properties.

## 5. Conclusion

A theory of time-dependent fluorescence spectrum for a polar solute in polar solvents is formulated and applied to C153 in acetonitrile in the present study. The dynamics of the fast motion of intramolecular vibration and the nonpolar collision-like interaction is assumed to be the same in nonpolar solvents and polar solvents and such motion is seen to decay rapidly. Polar solvents provide additional electrostatic interaction whose dynamics is slower and is observed in the experiments. On the basis this assumption, we have developed a method for including the vibronic transitions of the dye molecule in the time-dependent fluorescence spectrum, and the results for C153 in acetonitrile are close to experimental ones.

Since it is now possible to estimate the overall time-dependent spectrum, a presentation of the data for the time-evolution fluorescence spectrum in numerical form, rather than only a fitted analytic functional form, would remove the added approximation of the fitting.

**Acknowledgment.** We wish to particularly thank Professor J. E. Bertie for providing the data file and the computer code on the dielectric dispersion of acetonitrile before publication. It is a pleasure to acknowledge the support of the National Science Foundation and the Office of Naval Research. Y.G. would like to acknowledge the support of the James W. Glanville Postdoctoral Scholarship in Chemistry at Caltech and the support in the early stages of this research by a Rueff-Wormser Fellowship.

## References and Notes

- Bakhshiev, B. G. *Opt. Spectrosc.* **1964**, *16*, 446.
- Mazurenko, Y. T.; Bakshiev, B. G. *Opt. Spectrosc. (USSR)* **1970**, *28*, 490.
- Mazurenko, Y. T.; Udaltsov, V. S. *Opt. Spectrosc. (USSR)* **1978**, *44*, 417.
- Mazurenko, Y. T. *Opt. Spectrosc. (USSR)* **1980**, *48*, 388.
- Nee, T.-W.; Zwanzig, R. J. *Chem. Phys.* **1970**, *52*, 6353. van der Zwan, G.; Hynes, J. T. *J. Chem. Phys.* **1982**, *76*, 2993.
- Ware, W. R.; Lee, S. K.; Brant, G. J.; Chow, P. P. *J. Chem. Phys.* **1971**, *54*, 4729. Okamura, T.; Sumitani, M.; Yoshihara, K. *Chem. Phys. Lett.* **1983**, *94*, 339. Su, S.-G.; Simon, J. D. *J. Phys. Chem.* **1987**, *91*, 2693.
- Jarzęba, W.; Walker, G. C.; Johnson, A. E.; Kahlow, M. A.; Barbara, P. F. *J. Phys. Chem.* **1988**, *92*, 7039.
- Maroncelli, M.; Fleming, G. R. *J. Chem. Phys.* **1987**, *86*, 6221.
- Hornig, M. L.; Gardecki, J. A.; Papazyan, A.; Maroncelli, M. *J. Phys. Chem.* **1995**, *99*, 17311.
- Gardecki, J.; Hornig, M. L.; Papazyan, A.; Maroncelli, M. *J. Mol. Liq.* **1995**, *65-6*, 49.
- Maroncelli, M. *J. Phys. Chem.* **1997**, *106*, 1545.
- Kumar, P. V.; Maroncelli, M. *J. Chem. Phys.* **1995**, *103*, 3038.
- Jimenez, R.; Fleming, G. R.; Kumar, P. V.; Maroncelli, M. *Nature* **1994**, *369*, 471.
- Jarzęba, W.; Walker, G. C.; Johnson, A. E.; Barbara, P. F. *Chem. Phys.* **1991**, *152*, 57.
- Castner, E. W., Jr.; Maroncelli, M.; Fleming, G. R. *J. Chem. Phys.* **1987**, *86*, 1090.
- Maroncelli, M.; Castner, E. W., Jr.; Bagchi, B.; Fleming, G. R. *Faraday Discuss. Chem. Soc.* **1988**, *85*, 199.
- Castner, E. W., Jr.; Fleming, G. R.; Bagchi, B. *Chem. Phys. Lett.* **1988**, *143*, 270.
- Wolynes, P. G. *J. Chem. Phys.* **1987**, *86*, 5133. Rips, I.; Klafter, J.; Jortner, J. *J. Chem. Phys.* **1988**, *88*, 3246; *Ibid.* **1988**, *89*, 4288. Nichols III, A. L.; Calef, D. F. *J. Chem. Phys.* **1988**, *89*, 3783.
- Raineri, F. O.; Resat, H.; Perng, B.-C.; Hirata, F.; Friedman, H. L. *J. Chem. Phys.* **1994**, *100*, 1477. Zhou, Y.; Friedman, H. L.; Stell, G. *J. Chem. Phys.* **1989**, *91*, 4885. Fried, L. E.; Mukamel, S. *J. Chem. Phys.* **1990**, *93*, 932. Loring, R. F.; Mukamel, S. *J. Chem. Phys.* **1987**, *87*, 1272. Bagchi, B.; Chandra, A. *J. Chem. Phys.* **1989**, *90*, 7338.
- Maroncelli, M.; Fleming, G. R. *J. Chem. Phys.* **1988**, *89*, 875.
- Kahlow, M. A.; Jarzęba, W.; Kang, T. J.; Barbara, P. F. *J. Chem. Phys.* **1989**, *90*, 151.
- Bagchi, B.; Chandra, A. *Adv. Chem. Phys.* **1991**, *80*, 1. Bagchi, B. *Annu. Rev. Phys. Chem.* **1989**, *40*, 115.
- Roy, S.; Bagchi, B. *J. Chem. Phys.* **1993**, *99*, 9938.
- Nandi, N.; Roy, S.; Bagchi, B. *J. Chem. Phys.* **1995**, *102*, 1390.
- Biswas, R.; Nandi, N.; Bagchi, B. *J. Phys. Chem.* **1997**, *101*, 2968.
- Roy, S.; Komath, S.; Bagchi, B. *J. Chem. Phys.* **1993**, *99*, 3139.
- Gertner, B. J.; Whitnell, R. M.; Wilson, K. R.; Hynes, J. T. *J. Am. Chem. Soc.* **1991**, *113*, 74.
- Ladanyi, B. M.; Stratt, R. M. *J. Phys. Chem.* **1995**, *99*, 2502; *Ibid.* **1996**, *100*, 1266.
- Maroncelli, M.; Fleming, G. R. *J. Chem. Phys.* **1988**, *89*, 5044.
- Hsu, C.-P.; Song, X.; Marcus, R. A. *J. Phys. Chem. B* **1997**, *101*, 2546.
- Carter, E. A.; Hynes, J. T. *J. Chem. Phys.* **1991**, *94*, 5961.
- Rosenthal, S. J.; Jimenez, R.; Fleming, G. R.; Kumar, P. V.; Maroncelli, M. *J. Mol. Liq.* **1994**, *60*, 25.
- Fonseca, T.; Ladanyi, B. M. *J. Phys. Chem.* **1991**, *95*, 2116.
- Ando, K.; Kato, S. *J. Chem. Phys.* **1991**, *95*, 5966.
- Zhu, J.; Cukier, R. I. *J. Chem. Phys.* **1993**, *98*, 5679.
- Georgievskii, Y.; Hsu, C.-P.; Marcus, R. A. *J. Chem. Phys.*, submitted.
- Loring, R. F.; Yan, Y. J.; Mukamel S. *J. Chem. Phys.* **1987**, *87*, 5840.
- Loring, R. F.; Yan, Y. Y.; Mukamel S. *Chem. Phys. Lett.* **1987**, *135*, 23.
- Mukamel, S. *Principles of Nonlinear Optical Spectroscopy*; Oxford University Press: New York, 1995.
- For example, Mahan, G. D. *Many-particle Physics*, 2nd ed.; Plenum Press: New York, 1990.
- Fee, R. S.; Milsom, J. A.; Maroncelli, M. *J. Phys. Chem.* **1991**, *95*, 5170.
- Fee, R. S.; Maroncelli, M. *Chem. Phys.* **1994**, *183*, 235.
- For example: Passino, S. A.; Nagasawa, Y.; Joo, T.; Fleming, G. R. *J. Phys. Chem.* **1997**, *101*, 725. Bardeen, C. J.; Shank C. V. *Chem. Phys. Lett.* **1994**, *226*, 310.
- Maroncelli, M., private communication.
- Bagchi, B.; Oxtoby, D. W.; Fleming, G. R. *Chem. Phys.* **1984**, *86*, 257.
- Kubo, R. *J. Phys. Soc. Jpn.* **1962**, *17*, 1100.
- Kubo, R. In *Fluctuation, Relaxation and Resonance in Magnetic Systems*; ter Haar, D., Ed.; Oliver & Boyd: Edinburgh, 1962; p 23. Kubo, R. *Adv. Chem. Phys.* **1969**, *15*, 101.
- We note incidentally that in the expansion leading to eq 17 the terms in  $t_1^2$  and  $t_2^2$  each canceled and there was no  $t_1 t_2$  term.
- With eq 24 and refs 51 and 52, the absorption spectrum is written as the Fourier transform of  $\tilde{g}(\tau)$ . If the high-temperature approximation described in eq 27 and footnote 54 is used for the integrated correlation



function  $\zeta_f(\tau)$  (so that  $\zeta_f(\tau) \approx \lambda_f k_B T \tau^2$ ), then the Fourier transform of  $\tilde{g}(\tau)$  in eq 24 is

$$g(\omega) \sim \exp \left[ - \frac{(\Delta G_{np}^{\circ} - \hbar\omega + \lambda_f)^2}{4\lambda_f k_B T} \right]$$

The above expression is of the same form as the activation factor in the rate expression of nonadiabatic electron-transfer reactions (cf.: Marcus, R. A.; Sutin, N. *Biochim. Biophys. Acta* **1985**, 811, 265) if the quantity  $\lambda_f$  replaces the reorganization energy  $\lambda$  in electron-transfer reactions.

(50) In eqs 25 and 8, the integration limits for the time variables  $\tau''$  and  $u$  have been moved to positive and negative infinities, because the integration upper bound  $t$  for the old variables  $t_1$  and  $t_2$  is assumed to be much larger than the width of pump pulse profile  $\tau_p$ . Thereby, with the majority of the excitation process occurring at short times ( $\tau_p$ ), the integration limits for both  $t_1$  and  $t_2$  can be reasonably approximated as  $-\infty$  to  $\infty$  and so can the limits for  $\tau''$  and  $u$ .

(51) Lax, M. *J. Chem. Phys.* **1952**, 20, 1752.

(52) In ref 51 the absorption and emission spectra are shown to be the Fourier transformation of their time-dependent characteristic functions (eq 8.20). Expressions in eqs 23 and 24 are such characteristic functions (they correspond to eqs 8.13 and 8.11 of ref 51, respectively.).

(53) The Fourier transformation of  $\theta(\tau') \tilde{f}(\tau')$  is a complex-valued function whose real part is the Fourier transformation of  $\tilde{f}(\tau')$  because

$$\tilde{f}(-\tau') = \tilde{f}^*(\tau')$$

where  $*$  denotes a complex conjugate. Such a time-reversal property arises from the similar property for the autocorrelation function  $\langle X_f(t) X_f(0) \rangle$  (cf. eqs 23 and 13):

$$\langle X_f(t) X_f(0) \rangle^* + \langle X_f(0) X_f(t) \rangle = \langle X_f(-t) X_f(0) \rangle$$

The first equality can be shown by taking the Hermitian conjugate (denoted as  $\dagger$  below) of the operators inside the thermal average, with the time-evolution of  $X_f(t)$  being replaced by  $U(t)^\dagger X_f(0) U(t)$ , where  $U(t)$  is the time-evolution operator which, when it operates on a wave function, propagates it forward for time  $t$ . The second equality makes use of the stationarity property.

(54) This crude short-time approximation for  $\zeta_s(t)$  can be seen by taking the  $\beta \rightarrow 0$  (high temperature) limit of the real part of the expression in eq 35 (with  $\coth \beta \hbar \omega / 2 \sim 2 / \beta \hbar \omega$ ) and then taking the leading term (which proves to be  $t^2$ ) of the Taylor expansion in time  $t$ . In simplifying this result, the expression for  $\lambda_s$  in footnote 66 was used. The imaginary part of the correlation function  $\langle X_s(t) X_s(0) \rangle$  is much smaller than its real part, at this high-temperature limit.

(55) Ovchinnikov, A. A.; Ovchinnikova, M. Ya. *Sov. Phys. JETP* **1969**, 29, 688.

(56) Abrikosov, A. A.; Gorkov, L. P.; Dzyaloshinski, I. E. *Methods of Quantum Field Theory in Statistical Physics*; Dover Publications, Inc.: New York, 1963.

(57) Caldeira, A. O.; Leggett, A. J. *Ann. Phys. (N.Y.)* **1983**, 149, 374.

(58) Mukamel, S. *J. Phys. Chem.* **1985**, 89, 1077.

(59) Georgievskii, Y.; Hsu, C.-P.; Marcus, R. A. Linear Response Theory Approach for Solvation Dynamics and Nonlinear Spectroscopy, in preparation.

(60) For example: Chandler, D. In *Liquids, freezing and glass transitions*; Hansen, J. P., Levesque, D., Zinn-Justin, J., Eds.; Elsevier Science: North-Holland, 1991; p 201.

(61) For example: Kubo, R.; Toda, M.; Hashitsume, N. *Statistical Physics*; Springer-Verlag: New York, 1983; Vol. II, Chapter 4.

(62) Onsager, L. *J. Am. Chem. Soc.* **1936**, 58, 1486.

(63) Böttcher, C. J. F. *Theory of Electric Polarization*, Elsevier: Amsterdam, 1983; Vol. 1.

(64) van der Zwan, G.; Hynes, J. T. *J. Phys. Chem.* **1985**, 89, 4181.

(65) Mazurenko, Y. T. *Opt. Spectrosc. (USSR)* **1974**, 36, 283.

(66) In eq 37, it is seen that the second term vanishes as  $t \rightarrow \infty$ . If the expression for  $\lambda_s$  is similar to that for  $\lambda_f$  in eq 21, then the first term of eq 37 should be  $-\lambda_s \hbar$ . Namely

$$\lambda_s \left( = - \frac{1}{\hbar} \lim_{t \rightarrow \infty} \text{Im} \zeta'_s(t) \right) = \frac{1}{\pi} \int_0^\infty d\omega \frac{J(\omega)}{\omega}$$

(67) Barthel, J.; Bachhuber, K.; Buchner, R.; Gill, J. B.; Kleebauer M. *Chem. Phys. Lett.* **1990**, 167, 62.

(68) Barthel, J.; Kleebauer M.; Buchner, R. *J. Solut. Chem.* **1995**, 24, 1.

(69) Arnold, K. E.; Yarwood, J.; Price A. H. *Mol. Phys.* **1983**, 48, 451.

(70) Ikawa S.; Ohba, T.; Tanaka, S.; Morimoto, S. Fukushi, K.; Kimura, M. *Int. J. Infrared Millimeter Waves* **1985**, 6, 287.

(71) Fujita, Y.; Ohba, T.; Ikawa S.-I. *Can. J. Chem.* **1991**, 69, 1745.

(72) Ohba, T.; Ikawa, S. *Mol. Phys.* **1991**, 73, 985.

(73) Firman, P.; Marchetti, M.; Xu, M.; Eyring, E. M.; Petrecci, S. *J. Phys. Chem.* **1991**, 95, 7055.

(74) Goplen, T. G.; Cameron, D. G.; Jones, R. N. *Appl. Spectrosc.* **1980**, 34, 657.

(75) Bertie, J. E. *J. Phys. Chem. B* **1997**, 101, 4111.

(76) The absorption coefficients reported in ref 70 are in good agreement with results from Arnold et al.<sup>69</sup> if the latter were scaled downward by 7%. That scaled profile, as shown in ref 70, is in good agreement with the results later reported in refs 71 and 72. Since only a few numerical data are available for those results, the overall spectrum in the present work is obtained from the curve in Figure 6 of ref 70 representing the scaled results of Arnold et al.

(77) Press, W. H.; Flannery, B. P.; Teukolsky, S. A.; Vetterling, W. T. *Numerical Recipes*; Cambridge University Press: Cambridge, 1986.

(78) In the present calculation, the data available from refs 67, 70, 73, and 75 have three "blank" regions: from 3 to 10, 220 to 320, and 430 to 700  $\text{cm}^{-1}$ . We assume that for those regions,  $k(\tilde{\nu})$  can be approximated by smooth curves without any peaks. For the lowest frequency region, in order to avoid the oscillation artifact arising from the cubic spline fit, the spline fit and interpolation are performed at the logarithm scale of both  $k$  and  $\tilde{\nu}$  for the data under 30  $\text{cm}^{-1}$ .

(79) For example: McQuarrie, D. A. *Statistical Mechanics*; Harper & Row: New York, 1976; pp 498–499.

(80) Bertie, J. E.; Lan, Z. *J. Chem. Phys.* **1995**, 108, 10152. The numbers in the row denoted as "Eq.(3)+” of Table IV are used.

(81) At the lower frequency limit, there is a small but noticeable difference ( $\leq 0.1$ ) in calculated  $n$  (eq 41) and those given by taking the real part of the square root of  $\epsilon(\omega)$  given by the Cole–Cole equations in ref 67. It may arise from the errors of extracting data from figures in the literature<sup>70,75</sup> and the subsequent use of a spline fit to represent the real spectrum or from the assumptions used to fill in the regions where the absolute absorption spectra are not available.<sup>78</sup> For the present work a linear combination of the refractive index predicted from the Cole–Cole equation ( $n_{\text{Cole}}$ ) and the Kramers–Kronig integration ( $n_{\text{KK}}$ ),  $n = w n_{\text{Cole}} + (1 - w)n_{\text{KK}}$  is assumed, with a weighting factor  $w$  that varies linearly from 0 at  $\tilde{\nu} = 3 \text{ cm}^{-1}$  to 1 at  $\tilde{\nu} = 5 \text{ cm}^{-1}$ .

(82) Formally, the quantity  $(\Delta G^{\text{solv}} + \lambda_s)/\hbar$  is the difference in the position of the absorption spectra in nonpolar and polar solvents, if the solute were a simple two-state system. For molecules as complicated as C153, it can be obtained as follows: The absorption spectrum in a polar solvent can be estimated as<sup>4,41,42</sup>

$$g_p(\omega) = \int_{-\infty}^{\infty} d\omega' g_{np}(\omega - \omega') p_1(\omega')$$

where the absorption spectra in the polar solvent ( $g_p(\omega)$ ) and a nonpolar solvent ( $g_{np}(\omega)$ ) are related by a convolution over the inhomogeneous site distribution created by the polar environment. Hornig et al.<sup>9</sup> have used a Gaussian functional form for  $p_1(\omega')$  with its mean and variance adjusted to obtain the best agreement between the estimated and the experimental absorption spectrum in polar solvents, using the measured *nonpolar* absorption spectrum and the above equation. The desired quantity  $(\Delta G^{\text{solv}} + \lambda_s)/\hbar$  is then the averaged frequency change as described by the Gaussian probability  $p_1(\omega')$ , which is denoted by  $\delta_0$  in ref 9. The averaged spectral shift reported there is 1740  $\text{cm}^{-1}$  for acetonitrile. However, since the absorption and emission spectra in nonpolar solvents that are used for the present calculation are inferred from the figures in ref 9, the uncertainty from the inference is about 100  $\text{cm}^{-1}$ . We have adjusted the  $\delta_0$  reported there to 1490  $\text{cm}^{-1}$  in order to obtain the same zero-time estimation spectrum as that reported in ref 10, which does not depend on any dynamical quantities. (It depends only on this  $p_1(\omega)$ , the steady-state absorption and emission spectra in a nonpolar solvent (eq 2).)

(83)  $\lambda_s$  can be calculated using the expression discussed in footnote 66.

(84) Barthel, J.; Bachhuber, K.; Buchner, R.; Hetzenauer, H. *Chem. Phys. Lett.* **1990**, 165, 369.

(85) Bertie, J. E.; Zhang, S. L.; Eysel, H. H.; Baluja, S.; Ahmed, M. K. *Appl. Spectrosc.* **1993**, 47, 1100.

(86) Kindt, J. T.; Schmuttenmaer, C. A. *J. Phys. Chem.* **1996**, 100, 10373.

(87) Kovalenko, S. A.; Ruthmann, J.; Ernsting, N. P. *Chem. Phys. Lett.* **1997**, 271, 40.

(88) Raineri, F. O.; Perng, B.-C.; Friedman, H. L. *Electrochim. Acta* **1997**, 42, 2749.

(89) For example, Weiner, A. M.; Desilvestri, S.; Ippen, E. P. *J. Opt. Soc. B* **1985**, 2, 654. Bai, Y. S.; Fayer, M. D. *Chem. Phys.* **1988**, 128, 135. Joo, T.; Albrecht, A. C. *Chem. Phys.* **1993**, 176, 233. Meijers, H. C.; Wiersma, D. A. *J. Chem. Phys.* **1994**, 101, 6927. Bardeen, C. J.; Shank, C. V. *Chem. Phys. Lett.* **1994**, 226, 310.

(90) Nishiyama, K.; Okada, T. *J. Phys. Chem. A* **1997**, 101, 5729.